Advances in Astronomy and Space Physics, **8**, 28-33 (2018) doi: 10.17721/2227-1481.8.28-33

Probing the distant galaxy cluster JKCS 041 on the $L-T-M$ scaling relations

*Iu. V. Babyk**

Department of Physics and Astronomy, University of Waterloo, 200 University Avenue West, Waterloo, ON N2L 3G1, Canada
Main Astronomical Observatory of the NAS of Ukraine, 27 Akademika Zabolotnoho Str., 03143 Kyiv, Ukraine

The detailed X-ray analysis of the distant galaxy cluster JKCS 041 is presented. We use deep (~ 75 ks) archived data of X-ray Chandra Observatory to extract the main physical characteristic for one of the most distant galaxy cluster known to date. We investigate the imaging and spectral properties of JKCS 041. We explore its surface brightness, density, entropy, cooling time, and mass profiles. The temperature of JKCS 041 is equal to 7.4 ± 2.9 keV while the total virial mass is $M_{200} = (4.6 \pm 2.9) \times 10^{14} M_{\odot}$. The gas fraction is $\sim 10\%$ while the dark matter is $\sim 90\%$ at R_{200}.

We use the obtained physical parameters of JKCS 041 to build numerous X-ray scaling relations. By adding JKCS 041 parameters we increase the redshift of our previous cluster's sample from 1.4 to 1.8. We study the three classical relations between temperature, luminosity and total mass, and two additional. We find the concentration parameter of JKCS 041, build $c-M$ relation and compare them with current hydrodynamic simulations. In addition, we explore, for the first time in the case of distant objects, the $M - Y = T \cdot M_g$ relation which is one of the most robust mass estimators. We conclude that concentration parameter, c, of JKCS 041 is in a good agreement with theoretical predictions. The obtained X-ray scaling relations were used to probe their evolution. We find that our results show inconsistent with self-similar evolution models.

Key words: X-ray observations, distant galaxy clusters: JKCS 041

INTRODUCTION

Galaxy clusters are the biggest virialized objects in the Universe. They are significant objects for cosmological investigations providing constraints on some cosmological parameters. Galaxy clusters are comprised of thousands of individual galaxies which are permeated by dark matter and intracluster medium (ICM). The ICM is a hot, diffuse and optically thin plasma with a mean temperature of $kT = 2.0 - 15.0$ keV and density $\sim 10^{-3}$ cm^{-3}. The ICM includes heavy elements, with an abundance of 1/3 in solar units. The dark matter component of clusters is detected due to their gravitational influence on the ICM. Usually, optical observations are used to research the galactic component of galaxy clusters. The ICM provides an information about the temperature, metallicity, density, and flux of X-ray hot gas. These quantities are required to define a total mass of galaxy clusters. The evolution of the ICM is still under debate [23, 34], since different theoretical models are unable to describe observables of hot diffuse gas [4, 8, 9, 26, 27].

The X-ray scaling relations allow us to understand the evolution of X-ray hot gas (e.g. [6, 10, 11, 29]). Recent X-ray results reveal that the luminosity scales with temperature as $L \propto T^{2.7-3}$ for clusters [10, 17], $L \propto T^{3-4}$ for galaxy groups, and $L \propto T^{4-5}$ for massive, isolated early-type galaxies [7]. These scalings are much steeper than predicted by a self-similar model, $L \propto T^2$ [24]. According to the self-similar model, the internal shape of density profiles is independent of mass and redshift and should be invariant. The steepness of scaling relations is a significant indicator of non-gravitational processes, such as the feedback from active galactic nuclei (AGN), star formation, merger activity, and other, occur in the ICM. These processes must be taken into account for the robust evolution models.

The X-ray scaling relations that include total mass, M, are more fundamental due to the dependence of the derived cosmological parameters from the cluster total mass and relations with other cluster observables. To derive the cluster mass, it is necessary that scaling relations between main physical observables and total mass are calibrated. Furthermore, a low scatter in the determination of scaling

*babikyura@gmail.com

relations is desirable. The $L-T$ relation has a large intrinsic scatter, while the $M-T$ relation presents a considerably smaller scatter [7].

One of the robust ways to probe the evolution of hot gas in clusters is studying the X-ray scaling relations and their evolution in a wide range of redshifts. According to the ΛCDM theory, galaxy clusters are formed at the epoch when $z \sim 2$. Thanks to the latest generation of X-ray space telescopes, galaxy clusters at $z > 1$ have been detected. Here, we present the analysis of an archival observation of Chandra JKCS 041 galaxy cluster, where X-ray emission is detected at $z \sim 1.8$. JKCS 041 is one of the most distant clusters detected in X-ray to date. We study the main thermodynamic properties of this cluster, such as temperature, luminosity, entropy, cooling time, etc. We also investigate the distribution of X-ray total mass within three scaling radii, R_{2500}, R_{500} and R_{200}[1]. We use estimated physical parameters of JKCS 041 and our previous results of X-ray scaling relations within $0.1 < z < 1.4$ [10, 11] to explore these relations by adding the new result for the distant JKCS 041 cluster. In addition, we define a concentration parameter, c, of JKCS 041 and investigate $c-M$ distribution as well.

We use the following cosmological parameters: $\Omega_\Lambda = 0.73$, $\Omega_m = 0.27$, and $H_0 = 70\,\mathrm{km\,s^{-1}\,Mpc^{-1}}$.

X-RAY DATA ANALYSIS

JKCS 041 was observed by Chandra, during 75 ks (ObsID 9368) using ACIS-S instrument. To analyze X-ray data the `CIAO` software package (version 4.6) was used with latest calibration files. The data reduction and analysis were made in a similar way as given in our recent papers [5, 6, 10, 11]. We extract an image of JKCS 041 in 0.3 – 2.0 keV energy band, which provides the maximum ratio of signal to noise [1]. We exclude the point sources using `wavdetect` routine. All observable parameters were extracted within the smaller circular region shown in Fig. 1 (the left panel). The size of this region was chosen as $36.6''$ to be in consistency with the previous result of [1]. We extract the source and background spectra using `specextract` task. The background spectrum was extracted from a larger circular area shown in Fig. 1. We fit the cleaned source spectrum using `XSPEC` with a `phabs*apec` model [35] in the 0.3 – 5.0 keV energy band. The spectrum was grouped with 20 counts per bin using `grppha` tool. The obtained spectrum and the best-fit thermal model are shown in Fig. 1 (the right panel). The quoted spectral model fits observed spectrum well, showing $\chi^2 = 1.1$ for 17 degrees of freedom. During fitting, we fixed the metal abundance as 0.3 in solar units, the column density as $2.63 \times 10^{20}\,\mathrm{cm^{-2}}$ [18], and the redshift as 1.8.

We find the temperature of JKCS 041 to be 7.4 ± 2.9 keV, a bolometric luminosity of $(7.2 \pm 1.9) \times 10^{44}\,\mathrm{erg\,s^{-1}}$, and an absorbed bolometric flux in the 0.3 – 5.0 keV energy band of $(1.5 \pm 0.5) \times 10^{-14}\,\mathrm{erg\,cm^{-2}\,s^{-1}}$. The obtained temperature was used to calculate the R_{2500}, R_{500}, and R_{200} using the scaling relation of [33]. We find $R_{2500} = (192 \pm 36)$ kpc, $R_{500} = (480 \pm 44)$ kpc, and $R_{200} = (894 \pm 121)$ kpc. The errors of T, L and flux include uncertainties on the normalization of the used spectral model. Our temperature and luminosity results are in agreement with previous estimates of [1, 30].

The surface brightness profile was derived from the source region using `Sherpa` environment in the `CIAO` software package. We used a single β-model [16] to fit the obtained surface brightness profile in the form

$$S(r) = S_0\left(1+\left(\frac{r}{r_c}\right)^2\right)^{-3\beta+1/2} + C,$$

where $S(r)$ is the X-ray surface brightness as a function of projected radius, r_c is the core radius, and β is the slope of surface brightness profile. S_0, r_c, β, and C were free parameters in the model. We find $\beta = 0.48 \pm 0.12$ and $r_c = 290 \pm 46$ kpc as the best-fitting parameters with $\chi^2 = 1.6$. The derived surface profile and best-fit model are given in Fig. 2. The gas density profile was determined using the β-model parameters fitted to the X-ray surface brightness profile. The gas density for the β-model is

$$\rho_{\mathrm{g}}(r) = \rho_0\left(1+\left(\frac{r}{r_c}\right)^2\right)^{-3\beta/2}, \qquad (1)$$

where $\rho_0 = 2.21\mu m_p n_0$ is the central gas density. The central concentration, n_0, can be calculated from emissivity, ϵ, as

$$n_0 = \left[\frac{S_0}{r_c \epsilon B(3\beta-0.5, 0.5)}\right]^{0.5},$$

where $B(a,b)$ is the validity of the beta function (see [20] for more details).

We also derived the total gravitational mass assuming spherical symmetry and assuming that the hot gas is in hydrostatic equilibrium. For a gas in hydrostatic equilibrium,

$$\frac{\mathrm{d}P}{\mathrm{d}r} = -\frac{GM(r)}{r^2}\rho_{\mathrm{g}}(r),$$

where P is the gas pressure, G is the gravitational constant, ρ_{g} is the gas density, and M is the total mass inside a sphere of radius r. The gas pressure is related to the gas density and temperature through

[1] R_{2500}, R_{500}, R_{200} are radii within which the mean density is 2500, 500 or 200 times the critical density at the cluster redshift.

the ideal gas law, $P = \rho_g kT(r)/\mu m_p$. The total gravitating mass can then be written as

$$M(r) = -\frac{kT(r)r}{G\mu m_p}\left(\frac{\mathrm{d}\ln\rho_{\rm g}}{\mathrm{d}\ln r} + \frac{\mathrm{d}\ln T}{\mathrm{d}\ln r}\right),$$

where $\mu = 0.62$ is the mean molecular weight of the gas and m_p is the proton mass. Assuming that the gas is isothermal with a mean temperature T, the total mass of JKCS 041 can be expressed as

$$M = -\frac{kTr}{G\mu m_p}\left(\frac{\mathrm{d}\ln\rho_g}{\mathrm{d}\ln r}\right).$$

The gas mass was determined by integrating the gas density profile (see Eq. (1))

$$M_{\rm g} = 4\pi\rho_0\int_0^r r^2\left(1+\left(\frac{r}{r_c}\right)^2\right)^{-3\beta/2}\mathrm{d}r.$$

We use the averaged temperature, 7.4 ± 2.9 keV, and derived density profile to build an entropy profile of JKCS 041 as $K = k_B T/n_e^{2/3}$, where, n_e and T are the electron density and temperature of the cluster respectively, and k_B is the Boltzmann constant. The derived entropy profile of JKCS 041 is presented in Fig. 2. We find the central values of gas entropy as $\sim 10\,\mathrm{keV\,cm^2}$ which is consistent with low-redshift cool-core clusters. The hot diffuse gas inside the JKCS 041 emits away its thermal energy after some time. This time is called the cooling time and can be obtained by $t_{cool} = 3P/[2n_e n_H\Lambda(Z,T)] = 3PV/2L$, where $\Lambda(Z,T)$ is a cooling function that depends on metallicity, Z, and temperature, T, while P is the pressure, and L is the X-ray luminosity. The central cooling time is 1 Gyr indicating that JKCS 041 hosts a cool core. The obtained cooling time profile is shown in Fig. 2 as well.

We used the scaling relation of [33] to define scaling radii as $R_{2500} = (192 \pm 36)$ kpc, $R_{500} = (480 \pm 44)$ kpc, and $R_{200} = (894 \pm 121)$ kpc. The total mass of JKCS 041 cluster within these radii is $M_{2500} = (3.1 \pm 1.8) \times 10^{13} M_\odot$, $M_{500} = (2.6 \pm 2.2) \times 10^{14} M_\odot$ and $M_{200} = (4.6 \pm 2.9) \times 10^{14} M_\odot$. The gas mass is equal $M_{g_{2500}} = (8.3 \pm 4.4) \times 10^{12} M_\odot$, $M_{g_{500}} = (2.4 \pm 1.4) \times 10^{13} M_\odot$ and $M_{g_{200}} = (3.1 \pm 1.8) \times 10^{13} M_\odot$ at R_{200}. The fraction of hot gas is $\sim 10\%$, while the dark matter is $\sim 90\%$ within R_{500} and R_{200}. In the case of R_{2500}, the gas fraction is about 30% that is consistent with theoretical predictions of structure formation [21, 22].

We also define a concentration parameter, c, of JKCS 041 as $c \equiv R_{500}/r_s$. The scale radius, r_s, was taken from [32], where authors built $T - r_s$ scaling relations for a large sample of galaxy clusters. We found $r_s = 90.0 \pm 2.6$ kpc for the JKCS 041, and found c_{500} to be 5.4 ± 0.6. The left panel in Fig. 3 illustrates where JKCS 041 lies on the $c_{500} - M_{500}$ relation, suggested by hydrodynamic simulations of [19]. It is important to note that we convert the concentration and mass of JKCS 041 according to the [19] cosmological parameters. We also used the 2σ scatter in the concentration parameter typically found in numerical simulations obtained by [37] with $\sigma_{\ln c} = 0.22$.

We then constructed $M - Y$ scaling relation for JKCS 041 and compared them with previous results. The $M - Y$ relation is proposed by [25] as one of the most robust X-ray mass estimators. The Y quantity is defined as

$$Y = T \times M_{gas}. \quad (2)$$

[28] performed hydrodynamic simulations to determine the total thermal energy, Y, and found that this relation (see Eq. (2)) gives much smaller scatter for total mass within fixed Y then the $M - T$ scaling relation. In addition, they showed that $M - Y$ relation is not so sensitive to cooling, and AGN feedback.

The Y of JKCS 041 is equal to 17.76 in units (keV$\times 10^{13} M_\odot$). The $M - Y$ scaling relation obtained by [36] is shown in Fig. 3 (the right panel) with our JKCS 041 result and those presented in [1]. Both results provide slightly lower values compared to the low-redshift results taken from [36]. According to the self-similar model, the $M - Y$ scaling relation can be fitted using the power law with the slope of 3/5. We took two lines of fit (Fit1 and Fit2) from [36] for clusters with low redshifts. The Best Fit Model line corresponds our power law fit as $M \propto Y^{0.66 \pm 0.07}$ that is consistent with the self-similar model.

THE X-RAY SCALING RELATIONS

The derived physical properties of the hot gas of JKCS 041 have been compared with previous results of 22 clusters in the $0.01 < z < 1.41$ redshift band found in a series of our previous papers [5, 6, 10, 11]. Firstly, we built $L - T$ scaling relation with JKCS 041 results, and those estimates made by [2] as well (see left panel in Fig. 4). We used the same normalization and slope parameters in $L_g \sim (1+z)^{A_{LT}} T^{\beta_{LT}}$ fit as $A_{LT} = 1.50 \pm 0.23$ and $\beta_{LT} = 2.55 \pm 0.07$ to model all data points in the sample. This result is consistent with our recent best-fit model. We also plot two self-similar models derived theoretically for the clusters at $z = 1.41$ and 2.2. [2] and our results lie below theoretical models by a factor 3.5. On the other hand, both of them are about 1.6σ away from our previous observed scaling relation, and 2.6σ from theoretical relations. We found that the probability to obtain these two points for 1.6σ away from our fit is only 7 percent, and for 2.6σ is 12 percent.

We also add the $M - T$ results of JKCS 041 to check the consistency with previous results and those obtained by [1]. To compare the evolution of our sample we image the models obtained by [37] and [3] (see right panel in Fig. 4). Both these fits were done for the high-z samples of galaxy clusters ($1 < z < 2$). [37] fit the observed $M - T$ relation as

$$M = M_5\,(T/5\,\mathrm{keV})^{\alpha}\,.$$

The best-fit slope of this model is 1.58 [37] which is smaller compared to our results. [3] nearly obtained the same slope as our results, while also finding a much higher normalization in the $M - T$ relation. In both cases, the self-similar evolution of the normalization is expected to follow

$$\frac{M_{\Delta}}{T^{3/2}} \propto E(z)^{-1}, E(z) = \frac{H(z)}{H_0}, \tag{3}$$

where Δ corresponds to the mass at R_{2500}, R_{500}, or R_{200}.

Our normalization is in very good agreement with present XMM-Newtond samples [31–33] and with those normalization results obtained in recent numerical simulations by [12, 13].

SUMMARY

Using Chandra observation, we derived the main physical characteristics for one of the most distant galaxy clusters, JKCS 041. We used these observables to probe the evolution of X-ray scaling relations over a wide range of redshifts. By adding X-ray properties of JKCS 041, we increased our previous range of redshifts to ~ 1.8. The combined sample of clusters within $0.1 < z < 1.8$ demonstrate strong evidence that galaxy clusters do not follow self-similar models over ~ 12 Gyr, confirming previous results and numerical simulations [10, 11, 14]. The obtained uncertainties from self-similarity can be explained by adding non-gravitational processes such as AGN feedback, radiative cooling, star formation, etc.

Here, we showed the constraints on the $L - M$, $M - T$, $c - M$, and $M - Y$ relations of hot diffuse gas in distant galaxy cluster JKCS 041. All our measurements are in a good agreement with previous calculations. Our mass results are consistent with recent papers, where authors found cluster mass using different methods, e.g., using the $\log M_{200}/M_{\odot}$ relation and X-ray temperature [36] found the total mass of JKCS 041 as $\log M_{tot} = 14.6$. Assuming the baryon fraction in the gas fraction, [2] found the total mass as $\log M_{200}/M_{\odot} = 14.2$.

The evolution of presented scaling relations is sensitive to cosmological parameters [10]. It's been observed that sampled high-redshift clusters show stronger dependencies between temperature, mass, and luminosity than low-redshift objects. We concluded that derived X-ray scaling relations consist with the preheating scenario presented in recent theoretical works [15, 21, 23, 26, 34].

ACKNOWLEDGEMENT

This research was carried out using the data obtained from the Chandra Data Archive and the Chandra Source Catalog, and software provided by the Chandra X-ray Center (CXC) in the application packages `CIAO`, and `Sherpa`. The author wishes to thank all the staff members involved in the Chandra project. The HEASARC on-line data archive at NASA/GSFC and ADS facilities have been used extensively in this research work.

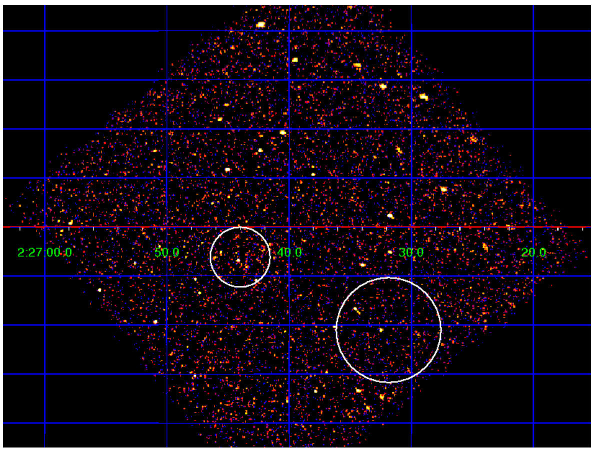

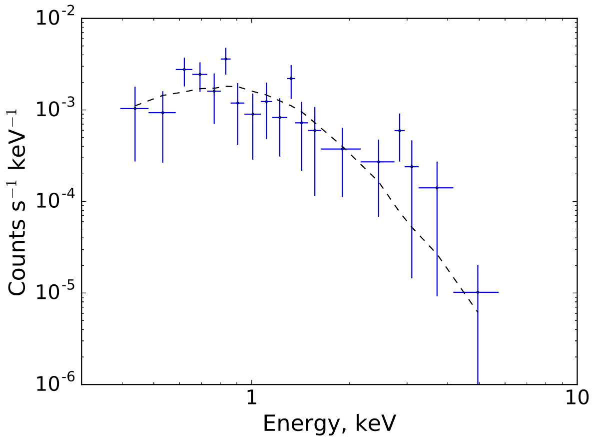

Fig. 1: The X-ray 0.3 – 2.0 keV image of JKCS 041 with equatorial coordinates and with two circular regions related to the source and background regions (left). The spectrum of JKCS 041 modeled by thermal model in the range of 0.3 – 5.0 keV (right).

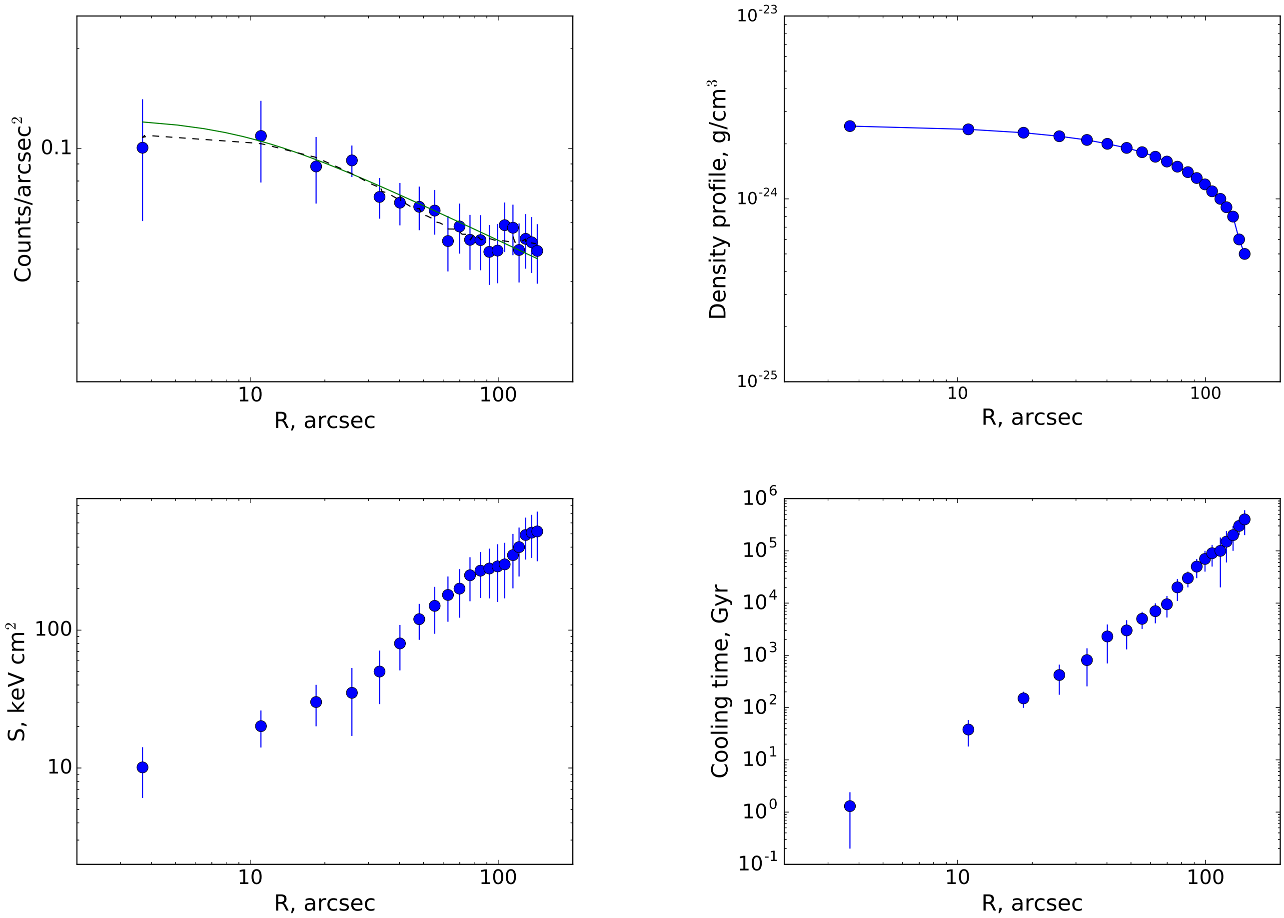

Fig. 2: The surface brightness profile of JKCS 041 (top left) with our β-model fit (solid line) and with previous [1] model (dashed line). The derived density (top right), entropy (bottom left), and cooling time (bottom right) profiles of JKCS 041.

REFERENCES

[1] Andreon S., Maughan B., Trinchieri G., Kurk J. 2009, A&A, 507, 147.

[2] Andreon S., Newman A. B., Trinchieri G. et al. 2014, A&A, 565, A120.

[3] Arnaud M., Pointecouteau E., Pratt G. W. 2005, A&A, 441, 893.

[4] Babyk Iu. V. 2012, Bulletin of the Crimean Astrophysical Observatory, 108, 87.

[5] Babyk Iu. V. 2014, Baltic Astronomy, 23, 93.

[6] Babyk Iu. V., Del Popolo A. 2014, Baltic Astronomy, 23, 9.

[7] Babyk Iu. V., McNamara B. R., Nulsen P. E. J. et al. 2018, ApJ, 857, 32.

[8] Babyk Iu. V., Melnyk O., Elyiv A. 2012, Advances in Astronomy and Space Physics, 2, 56.

[9] Babyk Iu. V., Vavilova I. B. 2012, in *'Proc. Conference of Young Scientists of CIS Countries Fifty years of Cosmic Era: Real and Virtual Studies of the Sky'*, eds.: Mickaelian A. M., Malkov O. Y., Samus N. N., National Academy of Sciences of the Republic of Armenia (NAS RA), Yerevan, 162.

[10] Babyk Iu. V., Vavilova I. V. 2014, A&SS, 349, 415.

[11] Babyk Iu. V., Vavilova I. V. 2014, A&SS, 353, 613.

[12] Bondi M., Ciliegi P., Venturi T. et al. 2007, A&A, 463, 519.

[13] Bondi M., Ciliegi P., Zamorani G. et al. 2003, A&A, 403, 857.

[14] Borgani S., Murante G., Springel V. et al. 2004, MNRAS, 348, 1078.

[15] Cavagnolo K. W., Donahue M., Voit G. M., Sun M. 2008, ApJ, 683, L107.

[16] Cavaliere A. & Fusco-Femiano R. 1976, A&A, 49, 137.

[17] Del Popolo A., Hiotelis N., Peñarrubia J. 2005, ApJ, 628, 76.

[18] Dickey J. M., Lockman F. J. 1990, ARA&A, 28, 215.

[19] Dolag K., Bartelmann M., Perrotta F. et al. 2004, A&A, 416, 853.

[20] Ettori S. 2000, MNRAS, 318, 1041.

[21] Fabian A. C., Crawford C. S., Ettori S., Sanders J. S. 2001, MNRAS, 322, L11.

[22] Fabian A. C., Sanders J. S., Allen S. W. et al. 2003, MNRAS, 344, L43.
[23] Hogan M. T., McNamara B. R., Pulido F. A. et al. 2017, ApJ, 851, 66.
[24] Kaiser N. 1986, MNRAS, 222, 323.
[25] Kravtsov A. V., Vikhlinin A., Nagai D. 2006, ApJ, 650, 128.
[26] McNamara B. R. & Nulsen P. E. J. 2007, ARA&A, 45, 117.
[27] McNamara B. R. & Nulsen P. E. J. 2012, New Journal of Physics, 14, 055023.
[28] Nagai D., Vikhlinin A., Kravtsov A. V. 2007, ApJ, 655, 98.
[29] Norman M. L. 2010, [arXiv:1005.1100].
[30] Pacaud F., Pierre M., Adami C. et al. 2007, MNRAS, 382, 1289.
[31] Pointecouteau E., Arnaud M., Kaastra J., de Plaa J. 2004, A&A, 423, 33.
[32] Pointecouteau E., Arnaud M., Pratt G. W. 2005, A&A, 435, 1.
[33] Pointecouteau E., Silk J. 2005, MNRAS, 364, 654.
[34] Pulido F. A., McNamara B. R., Edge A. C. et al. 2018, ApJ, 853, 177.
[35] Smith G. P., Kneib J.-P., Ebeling H., Gzoske O., Smail I. 2001, ApJ, 552, 493.
[36] Vikhlinin A., Burenin R. A., Ebeling H. et al. 2009, ApJ, 692, 1033.
[37] Vikhlinin A., Kravtsov A., Forman W. et al. 2006, ApJ, 640, 691.

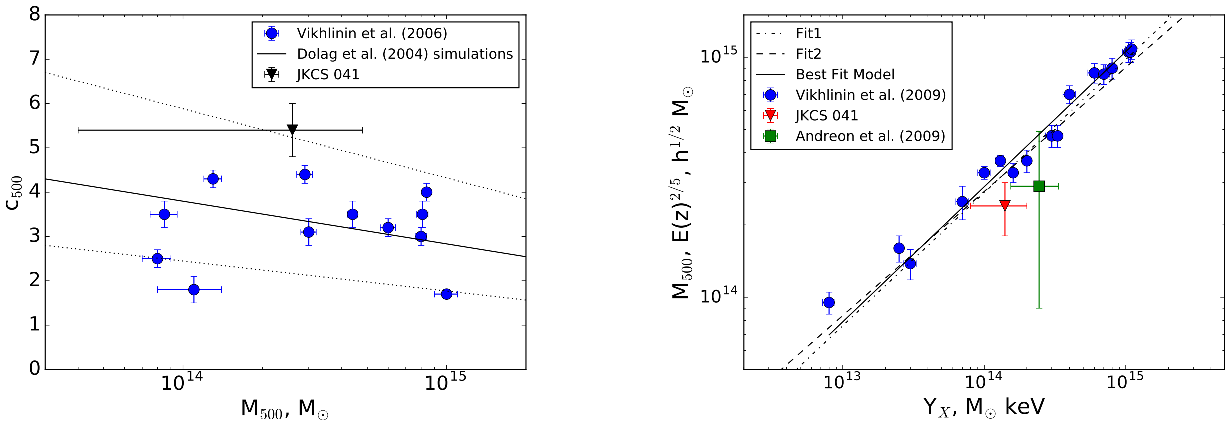

Fig. 3: $c-M$ relation of JKCS 041 (left) compared to previous results and simulations. Points with error bars performed by [37]. The solid line shows an average concentration of ΛCDM halos from hydrodynamic simulations of [19]. Dotted lines show 2σ scatter of concentrations at a fixed mass found in simulations. $M-Y$ relation of JKCS 041 (right). Crosses and their error bars demonstrate the Chandra result taken from [36]. The Fit1 line shows the model with a fixed slope, 3/5, at the self-similar value, while the Fit2 line corresponds to a power law modeling with the free value of slope ($\sim 0.52 \pm 0.11$). The Best Fit Model line corresponds to the modeling of all points with the free value of slope ($\sim 0.66 \pm 0.16$).

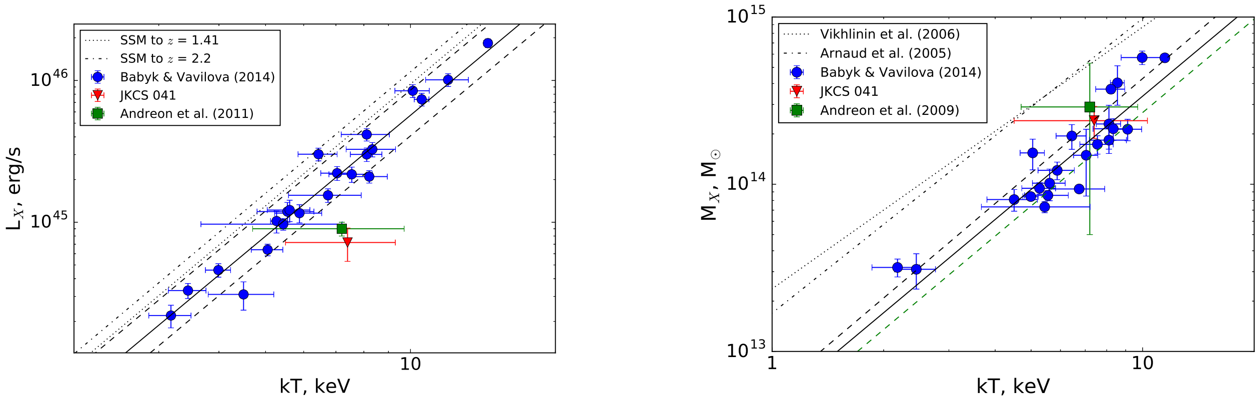

Fig. 4: $L-T$ relation for the sample of galaxy clusters, including JKCS 041 (left). The lines correspond to the $L_g \sim (1+z)^{A_{LT}} T^{\beta_{LT}}$ relation with $A_{LT} = 1.50 \pm 0.23$ and $\beta_{LT} = 2.55 \pm 0.07$ parameters obtained in [10]. $M-T$ relation (right). The lines correspond to the $M \sim (1+z)^{A_{MT}} T^{\beta_{MT}}$ relation with $A_{MT} = -0.58 \pm 0.13$ and $\beta_{MT} = 1.77 \pm 0.16$ parameters taken from [10]. The blue data points were taken from [11] with 1σ confidence level errors.